# "Numerical study of the sea breeze around Mallorca. Implications for the wave forecasts".

S. Ponce de León[1], A. Orfila[1], G. Vizoso[1], L. Renault[1], J. Tintoré[1,2]

[1] Department of Marine Technologies, Operational Oceanography and Sustainability (TMOOS), IMEDEA (CSIC-UIB), C/ Miquel Marqués 21, 07190, Esporles, Mallorca, Spain

[2] Coastal Ocean Observing and Forecasting System, Balearic Islands ICTS. Parc Bit, E-07121 Palma (Mallorca) Spain

**ABSTRACT**

A study of the marine breezes and their impact on the wave field around the Mallorca Island was carried out by numerical simulations. To perform this investigation, a spectral wave model SWAN and three different wind fields: WRF-Weather Research and Forecasting, HIRLAM-High Resolution Limited Area Model and ECMWF-European Center for Medium-range Weather Forecasts were used. The main characteristics of the modelled breeze circulation and its effects on the wave field are described. The modified wave field under breeze conditions in correlation with their variability and daily short life time period are studied and discussed from a physical point of view. The results show that the quality of a wave forecast will depend on the quality of the wind field and its ability to simulate the breezes; otherwise the anticipation of the modelled breeze spectral peak can occur. The study period covers the summers of 2009 and 2010.

***Keywords*:** *breezes; wind waves; Western Mediterranean Sea; Balearic Islands; Mallorca; WAM; SWAN; WRF; ECMWF; HIRLAM.*

**Corresponding Author*

Sonia Ponce de León

Marine Technologies, Operational Oceanography and Sustainability Department (TMOOS), Mediterranean Institute for Advanced Studies (IMEDEA), Spanish National Research Council (CSIC), University of Balearic Islands (UiB), Escoles Velles. C/ Miquel Marqués 21, 07190, Esporles, Illes Balears, Spain

Phone: 00 34 659027032
Fax: 00 34 971 61 17 61
Email: sponce@imedea.uib-csic.es

## 1. Introduction

Many studies have shown the existence of sea breezes in the coastal regions of mid-latitudes (Pavía and Reyes, 1983; Delgado-González et al., 1994; Fosberg and Schoeder, 1996). Sea breeze is a wind that develops over land near coastal areas. The mechanism of generation of these winds is the increase of the temperature differences between the land and sea which creates a pressure minimum over the land and, consequently, the cooler air from the sea blows inland. Wind velocities associated with the sea breezes may range from 5 up to 10 m/s or more.

The study of the breezes is of great importance because of the influence these winds have on the local wave field. Sea breezes induce changes in the incident wave field late morning (or early afternoon), increasing wave height and reducing wave period and changing also the wave propagation direction depending on the sea breeze (Masselink and Pattiaratchi 1998). Additionally, in areas where the sea breeze prevails the effect of these winds on the coastal dynamics could be considerable (Sonu and James 1973).

In the Mediterranean the major characteristics of sea breeze circulation systems were investigated by Papanastasiou et al. (2010) who, applying the WRF model (Weather Research Forecast) in the coastal zone of Greece, verified the ability of the atmospheric model to simulate adequately the wind field under breezes by calculating several statistical indices. In addition, they pointed out that the WRF simulations described satisfactorily circulation systems such as land and sea breezes.

In the Central Mediterranean basin the importance of the sea breezes in Calabria was characterized by Federico et al. (2010). Their study shows that breezes dominates the local circulation and play an important role in the local climate.

Marine breezes in the Balearic Islands were studied by Jansá and Jaume (1946) who described the sea breeze regime for the Mallorca Island. Later, Ramis et al., (1990), studied breeze circulation in Mallorca by a non-eulerian numerical model showing that the shape and topography of the Island determine the breeze's convergence in the centre of the island. Moreover, they indicated how the wind associated with the breeze flows around the Palma and Alcudia Bays (Fig. 1) and that at the East and West sides of the Island the breezes are weaker than in the bays.

The objective of this work is to investigate the effect of the marine breeze on the wave field around Mallorca by performing numerical simulations. A sea state characterization under simulated breeze conditions is given. A quantification of the

modelled wave field errors obtained from incomplete wind forcings (poor representation of breezes) is presented and discussed. The chosen period for the study has three months of duration covering the summer of 2009 (July and August) and 2010 (August).

According to the literature this is the first time that a spectral wave model (SWAN) is applied for studying the effect of the marine breezes on the wave field around a small island. The wave spectra estimated from observations and simulation in the present study were mainly classified as Wind Sea that refers to young waves under growth or in equilibrium with local wind. Wind wave with a fetch up to an equilibrium state is of particular importance for the development and verification of wave models. Moreover, a wind-wave-related research seeks an ideal sea state with no swell presence. In this sense, Mallorca Island and the sea breezes around it where the fetch is about 30-40 km is an ideal natural laboratory.

The paper is structured as follows. Section 2 reviews the area of study: the Mallorca Island in the Balearic Archipelago. Section 3 deals with the available observations in the area of study. Section 4 describes briefly the wave models and the numerical simulations set up. The marine breeze effect on the modelled wave field around Mallorca is given and discussed in Section 5. Finally, the concluding remarks are given in Section 6.

## 2. Study area

Mallorca is the largest of the Balearic Islands Archipelago near the eastern Mediterranean coast of Spain. The topography of the island is mainly characterized by the Tramuntana Mountains in the north-west side (1443 m of high), and smaller mountains to the east and in the centre of the island reaching 500 m of height. Two large bays located to the NE and to the SW also form part of the suitable breeze scenario: Alcudia and Palma Bays (Fig. 1). The Island is roughly square shaped of 65 km oriented SW, NE.

The topography of Mallorca determines the main features of the sea breeze such that around the Bay of Palma the wind blows from the South/South-West, where as at Alcudia Bay the breeze blows from the North East (Fig. 1).

From April to November and almost day by day during summer, the sea breeze is present (Ramis et al. 1990). In July and August the weather conditions are often almost

the same daily being this area an excellent scenario for the study of the sea breeze in small islands and associated mesoscale phenomena.

## 3. Observations

### *3.1 Buoys*

In situ measurements were available at two locations (B1 for 2009 and B2 for 2010, Fig.1) during the study period. Dragonera (B1) is a deep water buoy (135 m) located 20 km off the coast and operated by the Spanish Harbour Authority. This location is less affected by the sheltering effect of Mallorca Island (Ponce de León and Guedes Soares 2010) than the other buoys around the island. The second one, the Enderrocat buoy (B2) is located at 6 km from the coast in Palma Bay and operated by the IMEDEA (depth=28 m). Their locations are marked with triangles in Fig. 1; the geographical coordinates and depth of mooring are provided in Table 1.

The performance of the wave model was assessed with B1 and B2 data. In addition, a SWAN output grid point (circle #3 in Fig. 1) was selected for the local analysis of the modelled breezes impact in Alcudia Bay in the North of Mallorca. The SWAN spectra and source functions in the breezes summer period are analyzed in B2 (Fig. 1).

It is necessary to point out that B2 is a more suitable location for the analysis of the modelled and observed breezes than B1 which since it is far away from the coast the sea breezes if observed are masked with other signals.

### *3.2 Time series*

Wind records from buoy B2 for August 2010 (Fig. 2, top) exhibit a clear wind variability associated with breeze summer conditions. A five day period (1st-5th of August) shows a sinusoidal signal with a 12 hour period of the wind vectors (Fig. 2, middle panel). Land tends to heat and cool faster than sea surface and consequently a thermal difference arises which generates the breezes across the coastline. The wind flows towards the coast from early in the morning around 8 a.m. to 20 p.m. whereas the sea is calm. Later, at night, the breeze circulation pattern reverses giving rise to an opposite flow directed from land to the sea. A zoom for 1$^{st}$ of August show clear the behaviour of the breezes along a day (Fig. 2, bottom panel).

To visualize the temporal variability of the wind, a spectral analysis of measured wind speed time series at B2 was performed for a number of records of 4463 (1 month sampled at 10 minutes). A clear 24 h signal associated with this daily process can be seen in Fig. 3. The peak might be associated with a clear signal of the breezes. The spectrum was estimated averaging 2 adjacent frequency bands, resulting in a frequency bandwidth of 0.0248 cycles per hour (cph). Periods of minutes to several hours can be seen in the power spectral density of wind speed in Fig. 3 corresponding to diurnal and semidiurnal fluctuations. The spectral peaks at 0.043 and 0.08 cph (periods of 24 h, and 12 hours) are indicated with arrows. The associated wave spectrum from the recorded signal show simultaneously peaks in accordance with the wind spectrum.

## 4. Numerical simulation

### *4.1 Atmospheric models* (*WRF, ECMWF, HIRLAM)*

The wind fields used as forcing for the wave models come from three main sources: ECMWF (European Center for Medium Weather Forecast), HIRLAM (High Resolution Limited Area Model) and WRF (Weather Research and Forecasting).

ECMWF winds are data from the MARS (Meteorological Archival and Retrieval System) with a horizontal resolution of $0.13^{o}$ for the whole Mediterranean Sea every 6 hours. The ECMWF is a spectral model which incorporates a 4D-VAR assimilation procedure (Jung et al. 2005). Forecasts were provided every 6 hours with a horizontal resolution of 25 km until December 2009. The vertical structure of the atmosphere is solved by a multi-level hybrid sigma coordinate system (Simmons 2006). These winds have been interpolated in time to 1 hour to match with the input time step of the WAM output wave boundary conditions for the SWAN nested grid.

The HIRLAM is a hydrostatic, primitive-equation model which uses a 3D-VAR data assimilation scheme (Yang et al. 2005). In the Western Mediterranean, HIRLAM forecasts are supplied by the Spanish Meteorological Agency (AEMET) providing wind fields every 3 hours at 16 km (low resolution) and 5 km (high resolution) twice a day with a 72 h horizon (Sotillo et al. 2008). In this configuration, HIRLAM takes the boundary conditions from the ECMWF atmospheric global model.

The WRF (Skamarock et al. 2005; Skamarock et al. 2008) model is a next-generation mesoscale non-hydrostatic numerical weather prediction system designed to serve both

operational forecasting and atmospheric research needs. For this work, the simulation includes three two-way nested domains with horizontal grid spacing ($\Delta x = \Delta y$) of 30 km, 6 km and 1.5 km. Domain 1 (coarser mesh) covers the western Europe and North Africa (32.6°N - 44.8°N, 5°W - 8.6°E) whereas the nested domains cover the western Mediterranean sea (36.5°N - 42.2°N, 0.6°W - 5.9°E) and the Balearic Sea (38.6°N - 40.3°N, 1.6°W - 4.1°E). A total of 47 levels were used in the vertical, half of them in the lowest 1.5 km. The model coarse grid was spun-up and interpolated (using time-dependent boundary conditions) to the boundary of domain 1 from the NCEP (National Center for Environmental Prediction) - NCAR (National Center for Atmospheric Research) reanalysis every 6 h. This configuration provides forecasts with a temporal resolution of 1 and 3 hours.

*4.2 The spectral wave models WAM and SWAN*

WAM and SWAN are phase-averaged or spectral wave models that describe the evolution in time and space of the energy density wave spectrum F ($\sigma$, $\theta$), as a function of the relative angular frequency $\sigma$ ($=2\pi f$) and mean wave propagation direction $\theta$. A general form of the energy balance equation in Cartesian coordinates can be expressed as,

$$\frac{\partial F}{\partial t} + \frac{\partial}{\partial x}(c_x F) + \frac{\partial}{\partial y}(c_y F) + \frac{\partial}{\partial \theta}(c_\theta F) + \frac{\partial}{\partial \sigma}(c_\sigma F) = S_{tot} \qquad (1)$$

where $c_{x,y,\sigma,\theta}$ are the wave propagation components in the ($x, y, \sigma, \theta$) spaces.

Equations such as (1) are classed as energy transport equations and their solution requires the specification of appropriate initial and boundary conditions, an appropriate propagation scheme to represent the transport of energy within the computational domain and the specification of the forcing term or source functions (Young, 1999).

In general, $S_{tot}$ is represented as the summation of a number of the physical processes that can be modelled numerically, describing the development and the dissipation of the modelled waves in time and space,

$$S_{tot} = S_{wind} + S_{nl} + S_{ds} \qquad (2)$$

where $S_{wind}$ represents the wind input, $S_{nl}$ the non-linear wave-wave interactions and $S_{ds}$ the wave energy dissipation: whitecapping for deep water and bottom friction $S_{\mathrm{fric}}$ plus wave breaking $S_{br}$ for shallow waters.

In this study we adopt the wind speed at 10 metres, according to the actual version of the WAM model, based on the quasi-linear model for the sea surface boundary layer from Janssen (1989) and Janssen (1991).

The physical processes taken in to account in the hindcast SWAN simulations are wave generation by wind; nonlinear interactions between three and four spectral wave components; dissipation of wave energy by whitecapping and bottom friction dissipation based on the empirical JONSWAP model with a constant friction coefficient equal to 0.067 $m^2s^{-3}$.

The deep water wave model version was used for the WAM coarse grid, while for the high resolution SWAN model the spectral energy balance equation was integrated in the range from 0.04177 up to 1 Hz.

*4.3 Wave models set up*

Taking in to account that WAM is adequate for deep water and that the SWAN model accounts for the physical processes that take place in intermediate and shallow waters two modules are assumed: one for the generation of the waves, applying WAM, and a second one based on SWAN for wave transformation.

A coarse WAM wave model encompassing the Mediterranean basin was set to ensure the boundary wave conditions for a SWAN high resolution (dx=1500 m) nested grid around Mallorca Island (Fig. 1). For the WAM coarse wave model grid was implemented for 11245 grid points; for the SWAN nested grid the total grid points number was 18281. The grids geographical limits and other numerical parameters are compiled in Table 2. Different numerical simulations were performed using the different wind fields available for the wave forecast around the Balearic Islands (Table 3).

## 5. Results and discussions

*5.1 Influence of the sea breeze on the wave field*

The implications of the use of wrong wind field information (omission or poor representation of breezes) for a wave forecast in places where this phenomenon is of relative importance as on the case of Mallorca Island deserves attention for a correct wave forecast. A SWAN simulation was carried out using the HIRLAM(16) winds for

August 2010 summer. A comparison between the measured at B2 wind speed (u10) and significant wave height (Hs) against HIRLAM (u10) and the SWAN (Hs), respectively is given in Fig. 4. The wind speed was corrected to 10 m according the neutral logarithmic profile described in Bidlot et al. 2002. Some differences associated with omission of the breezes are obtained from the comparisons between measurements (U10 and Hs) and models. The wind speeds reach maximum values during midday hours; while the minimum values are observed during the late and early hours which are a typical behaviour associated with the local breeze.

Consequently, some errors are obtained on the modelled wave parameter (Hs) clearly associated with the inconsistencies on the modelled wind speed (top). These errors will have a direct impact on the computed SWAN Hs especially during the first 20 days of the month (bottom Fig. 4). The scatter index (SI-defined as the standard deviation of the predicted data with respect to the best-fit line, divided by the mean observations) and the best-fit line slope were calculated for August 2010. High scatter index for the Hs (0.4) and low best-fit slope (0.84) are obtained.

For 2009, the measured time series of wind and wave parameters versus hindcasted results were compared at B1 (Fig. 5) showing a good performance of the SWAN model. The high resolution atmospheric model WRF shows some overestimation of the wind speeds that induce enhanced Hs values. Similar scatter index for the Hs (0.35) and good slope (0.92) are obtained.

Considering the previous WRF wind field assessment studies of Papanastasiou et al. (2010) and Ponce de León et al. (2011) from which was shown that WRF data are suitable for the use under reasonable limits of the veracity, in the present study a temporal and spatial analysis of the breezes simulated with the WRF wind fields around Mallorca is performed for two months in the summer of 2009 for which the high resolution WRF winds were available.

A four days period (26-29th of July 2009) was chosen for the analysis of the impact of the modelled breezes (WRF(1.5)) on the SWAN computed wave field. The wind and wave propagation direction vectors are shown at B2 and B3 (Figures 6 and 7, respectively). As seen in Fig. 6 the fluctuation of the wind vectors (breezes) is in accordance (similar) with the previous measured wind during the summer of 2010 (Fig. 2). The effect of the WRF breezes on the wave field do not have an immediately

response and appears to be delayed. However, in Alcudia Bay (B3) the SWAN modelled wave direction seems to be less affected (Fig. 7, bottom panel).

In order to analyse spatially the performance of the models in simulating the classical breezes of Mallorca as described in Ramis et al., 1990 (sea breezes with wind speeds of 5-7 m/s blowing from the sea towards to the land in both Bays of Palma and Alcudia as represented in Fig. 1), a spatial evolution analysis of the hourly WRF atmospheric model winds during 26th of July 2009 is given starting from 11 UTC (Fig. 8). During the first hours of 26th (from the 00 up to 8 UTC) a gentle land breeze was observed in Palma Bay (wind speeds of about 5.5 m/s). The highest U10 value was observed to the NW of the Island that kept almost stationary during the next five hours. The sea breezes started around 10-11 a.m. when the wind turned from the sea to the land, and developed with time until approximately 20 UTC in the afternoon (Fig. 8)..

Hourly description in accordance with the breezes from the WRF winds behaviour and the associated wave field is compiled in Table 4. At 12 UTC the sea breeze wind speed was about 9.2 m/s (from the NE) in Alcudia, whereas in Palma Bay it was about 6 m/s (from the S, SW). These sea breeze conditions for this date induced a certain sea state (wave field) in Alcudia with Hs of 65 cm propagating from the NE (Fig. 9). At Palma Bay the calm persisted. “Spots” of the sea breezes can be distinguished around the Island. At 13 UTC, a similar situation such at 12 UTC, was observed but with a maximum value of wind speed located to NW of Mallorca, nearby Cabrera and at Alcudia Bay (Fig. 8). The sea state observed was similar as 1 hour before (Fig. 9). At 14 UTC the sea state kept the same sea breeze conditions at 13 UTC at Alcudia Bay. Hs higher than 30 cm were not observed (Table 4) in accordance with the low wind speed (6 m/s) observed in Palma Bay.

At 15 UTC the sea breezes develop and the wind speed reaches the maximum value of about 7-9 m/s in both Bays. From the WRF winds it was observed that the sea breeze at Alcudia is strong (9 m/s) than in Palma Bay (Fig. 8). From the simultaneous Hs wave field dated 26th of July at 15 UTC (Fig. 9), it can be seen that the maxima values are directly correlated with the sea breeze wind speed to the SE and NW of Mallorca (Fig. 8). However, low values of the Hs are observed from the hindcast at Palma Bay with typical values of 0.4 m (Fig. 9).

A different implication of the modelled breezes using WRF high resolution wind is that the variability associated with the sea breezes is not always reflected in the

computed wave field for those wind speeds lower than 7.5 m/s (Fig. 10). When the breezes develop to the East side of the Palma Bay (u10 about 7 m/s), low Hs values (aprox. 50 cm) can be observed in Palma Bay for 26th of July 2009 at 15 UTC (top left/right panels in Fig. 10). Whereas simultaneously, at Alcudia Bay higher Hs of about 0.9 m can be seen as the result of the breeze (u10 higher than 7.5 m/s). In addition, additional wave energy contribution can be observed coming from the East boundary.

It seems the computed wave field had insufficient time to grow as a response according to the short time scale of the breezes especially in Palma Bay. Sea breezes that can occur in short time scales and, having short duration, induce a highly dynamic effect that results in a wave field not having sufficiently time to develop. At this point, a numerical problem arises, when the SWAN model is applied in non stationary mode to this rapid change of the breezes. In order to avoid this numerical problem the calculations have been repeated for a smaller integration time step of 5 minutes to properly solve (or simulate) the dynamic growth.

The results with the lowest integration time step of 5 minutes (bottom left/right panels, Fig. 10) show higher Hs values inside the Palma and Alcudia Bay when compared with the first hindcasts performed with 30 minutes of time step (not shown). Moreover, the spatial variability is still the same for both simulations. Locally, where the buoy data information was available for the time series comparisons, no improvements in the adjustment were observed when the integration time step was reduced up to 5 minutes.

In addition, an interesting behaviour of the peak period (Tp) distribution was observed which exhibits a reduction of the Tp at the area where the sea breezes are observed, to the NW of Mallorca (left top panel of Fig. 10 and left panel of Fig. 11). In general, the peak periods range from 3 to 5 seconds in the region of the sea breezes indicating that mainly we are dealing with waves in equilibrium with the local wind.

From the WRF winds land breezes seem have an appearance of “spots” around the Mallorca Island including Palma Bay. Specifically, from WRF simulations a land breeze was observed (U10 maximum of 4-5 m/s, Fig. 12, left panel) with a large extent offshore on 5th of August of 2009 with a duration from 02 UTC up to 8 UTC in Alcudia Bay which reached the East side of Menorca Island (approximately 40 km of distance from the inner Alcudia Bay). However, no evidence in the associated wave fields

computed for the analyzed dates of the land breezes were found for those low wind speeds (4 m/s) as can be seen (Fig. 12, right panel) .

An investigation on the fetch and depth limited wave growth based on the 10 year data for two lakes in Holland and supplemented with SWAN model results reported that this model underestimated the quick response (within 0.3-1 h) to sudden wind change (Bottema and van Vledder, 2009).

High resolution wind forcing resolves quite well the local events in the Balearic Islands by evaluating the hindcasted Hs errors around Mallorca Island using the WRF high resolution (1.5 km) winds (Ponce de León et al., (2011)). For different locations around the island they obtained low biases and scatter index in accordance with other regional studies in the Western Mediterranean (Ardhuin et al., 2007).

*5.2 Influence of the sea breeze on the modelled wave spectra*

In order to further investigate the implications of the modelled WRF breezes on the hindcasted wave spectrum the hourly evolution of the 1D spectra estimated with the SWAN model (Fig. 13) for the location B2 (Palma Bay) is shown for 26th of July 2009. For the analysis the high frequency part of the wave spectrum are considered here as those frequencies higher than 0.2 Hz and up to 1 Hz.

In summer, the Balearic Sea is mainly dominated by "Wind Sea" generated by the local wind. Two peaked spectrum of relatively low energy at 11 and 12 UTC (Fig. 13), one of the peaks distributed at the high frequency part around 0.7 Hz (associated with the sea breeze) and the other at 0.2 Hz. As Ramis et al. 1990 have shown with a radiosonde ascent at 11 a.m. the see breeze circulation in Palma Bay is not yet fully developed at this time. Already at 13 UTC the secondary peak at high frequencies starts a redistribution of the energy towards the low frequencies.

At 14 UTC, the absolute spectral peak is distributed towards the low frequency part at 0.4 Hz; however the wave energy level is still low. From 14 UTC and until the end of the selected period for the analysis (26th of July at 22 UTC) a clear one peaked spectrum is established. The wave energy which dissipates with time starts to decrease at 18 UTC in the afternoon until the end of the chosen day (Fig. 13).

*5.3 The physics of the modelled wave under breeze conditions*

To facilitate the analysis from the physical point of view of the hindcasted spectra shown in Fig. 13 at B2, the associated Source Terms (SF) of Section 4.2 are represented for 26th of July 2009 (Fig. 14). The evolution of SF for the same dates as shown in Fig. 12 allows inferring that the high frequency secondary peak represents the beginning of the sea breeze at Palma Bay. The wave growth by the energy input of the wind ($S_{win}$) at 11 UTC has a relative importance at high frequencies in agreement with the beginning of the breeze and the bottom friction dissipation ($S_{fric}$) is important in the spectral low frequencies part. During the first hours of 26th of July, the wave spectra are dominated by the $S_{fric}$ (at low frequencies) and by the $S_{nl4}$ (at high frequencies) in the spectral balance.

At 12 UTC and 13 UTC, $S_{wind}$ and $S_{fric}$ have a similar role in the spectral domain. From 14 UTC, the nonlinear interactions play a major role in the redistribution of the wave energy towards the low frequencies (Fig. 13 and Fig. 14) inducing a single peak spectrum shape. At the same time $S_{wind}$ is the strongest process and $S_{fric}$ have a minor role in low frequencies. At 15 UTC, when the breezes are developed, a single peak wave spectrum centred at 0.4 Hz is observed as the result of the role of the $S_{nl}$ and $S_{wind}$ in the spectral balance. $S_{nl}$ becomes strong enough with time from 16 UTC up to 21 UTC, while whitecapping dissipation ($S_{wcap}$) is less important than $S_{wind}$. Later, at 17 UTC, the breeze is weak (6.6 m/s in Palma Bay), despite the $S_{wind}$ still having a wave energy redistribution role at high frequencies, as well as $S_{nl}$ and $S_{wcap}$. Finally, at 21 UTC, the $S_{wind}$ is weak enough and all the other physical processes determine the shape of the wave spectrum.

To gain a better insight on the influence of the marine breezes on the hindcasted wave field a comparison of the SWAN estimated wave spectra was done using the ECMWF(12.5)(solid line) and WRF(1.5)(dashed line) winds that are the forecast data used for the operational purposes.

The importance of the correct representation of the breezes to obtain a realistic wave spectra forecast under this local condition is shown in Fig. 15. SWAN one dimensional spectra obtained using both wind fields (ECMWF and WRF) are rarely coincident. From this fact it can be said that some times the ECMWF wind reproduces the breeze conditions at high frequencies as can be seen at the spectra dated 26th July at 06 and 12 UTC (Fig. 15). Considering that WRF winds have higher frequency in time (hourly)

these seem to be more suitable for the modelling of the breezes and their impact on the wave field.

Under breezes situation as shown in this study the effect of certain wind fields on the wave energy spectrum will have implications in a wave forecast. Depending of the wind field used in a wave forecast the effect on the obtained wave field will be different because the wind energy input will not be the same, which influences the different physical processes involved in the spectral energy balance.

Under breeze conditions the physical processes modulating the wave spectral balance represented in Fig. 16 and Fig. 17 for 26th July at 12 UTC and 27th July at 06 UTC, respectively, show that the intensity of the wind input ($S_{wind}$) contribution will vary depending on the wind field used. Consequently, all processes will differ depending of the ability of the atmospheric models for representing the breezes ($S_{wind}$). The use of the WRF and ECMWF wind fields will induce similar bottom friction dissipation ($S_{fric}$) (top and bottom Fig. 16) in the low frequency part for the 26th. However, non linear interactions ($S_{nl4}$) and the whitecapping dissipation ($S_{wcap}$) are more intensive using the ECMWF wind field (bottom) which produces and anticipated slightly reduced spectral wave energy peak (see the top second panel in Fig. 15). Whereas, for 27th July at 06 UTC, the behaviour obtained is differing. WRF "captures" better the breeze conditions as seen at the high frequency part (top panel in Fig. 17 and top 3$^{rd}$ and 4$^{th}$ panels in Fig. 15).

## 6. Conclusions

A spectral wave model (SWAN) was applied to assess the impact of the sea breezes on the hindcasted wave field in the Balearic Islands. A modification of the wave propagation direction in correlation with the breezes variability short life t span was obtained from the SWAN hindcast.

The main characteristics of the sea breeze circulation and its effects on the wave field were described and shown around the Mallorca using the WRF winds. The attention was focused in the two opposite bays located to the North (Alcudia) and South (Palma). From the simulations and the analysis it can be concluded that the WRF sea breezes in Alcudia Bay are more intense with a longer daily duration than in Palma Bay with the

consequent modification of the waves. The Alcudia Bay land breeze was not often observed but may reach the East coasts of Menorca Island.

WRF wind fields satisfactorily represent the local land-sea breezes around the Mallorca Island as described by Ramis et al. 1990 because this data has the high spatial resolution in time and space for representing the breezes. This fact reveals that WRF could be useful for a correct predictability of the presence and impact of the sea breeze leading to a more realistic sea state prediction in operational wave forecasts for the Balearic Islands in connection with the safety of the population in coastal zones. However, the ECMWF wind fields also represent with sufficient accuracy, but not always, the breezes as was shown in this study.

It can be concluded that SWAN model represents correctly the wave field under the marine breeze conditions when the wave model is forced with the high resolution (1.5 km) WRF winds. However, for certain breezes conditions, SWAN model resulted insensitive to short time scale breeze changes and to wind speeds lower than 7.5 m/s which usually are present in sea breezes, and consequently may affect the coastal wave forecast in the summer period.

Considering the present analysis it was concluded that WRF atmospheric model with the highest spatial resolution is suitable for the operational wave forecast around Mallorca where the breezes pattern have significance in the summer. However, the variability present in WRF wind is not free of errors as was shown in (Ponce de León et al 2011).

**Acknowledgments**

The authors would like to thank to Port Authority of Spain for providing the buoy data at Dragonera and to the ECMWF for the wind fields. Sonia Ponce de León is supported by funding from MICINN-(JDC).

## References


Ardhuin F., Bertotti L., Bidlot J.R. Cavaleri L., Filipetto V., Lefevre J.M., Wittmann P., 2007, Comparison of wind and wave measurements and models in the Western Mediterranean Sea, Ocean. Eng. 34, 526-541.

Bidlot J.R. , Holmes D.J., Wittmann P.A., Lalbeharry R., H.S. Chen H.S., 2002, Intercomparison of the performance of operational ocean wave forecasting systems with buoy data, Weather Forecasting 17, 287-310.

Bottema, M., Van Vledder, G.Ph., 2009, A ten-year data set for fetch- and depth-limited wave growth. Coastal Engineering 56, 703-725.

Booij, N., Ris, R.C., Holthuijsen, L.H., 1999, A third-generation wave model for coastal regions. 1. Model description and validation. Journal of Geophysical Research 104 (1999) 7649–7666.

Delgado O.E., Ocampo-Torres F.J., Larios Castillo S., 1994, Breezes during some months of spring and summer in the northwest of the Gulf of California. Ciencias Marinas 20(3), 421-440.

Federico, S., Pasqueloni, L., De Leo L., Belleci, C., 2010, A study of the breeze circulation during summer and fall 2008 in Calabria, Italy. Journal of Atmospheric Research 97, Issues 1-2, pp. 1-13.

Fosberg, M.A., Schroeder, M.S., 1996, Marine Air Penetration I Central California. J.A. Meteor. 5, 573-589.

Günther, H., Hasselmann, S., Janssen, P.A.E.M., 1992, The WAM model Cycle 4 (revised version), Deutsch. Klim. Rechenzentrum, Techn. Rep. No. 4, Hamburg, Germany.

Janjic, Z., Black, T., Pyle, M., Rogers, H., Chuang, Y., DiMego, G., 2005, High resolution applications of the WRF NMM. Extended abstract, 21st Conference on Weather Analysis and Forecasting. 17th Conference on Numerical Weather Prediction, American Meteorological Society, Washington, D. C., 21 pp.

Jansá, J.M., Jaume, E.,1946. The sea-breeze regime in the Mallorca Island (in spanish). Rev. Geofísica., 19, 304-328.

Jung, T., Klinker, K., Uppala, S., 2005, Reanalysis and reforecast of three major European storms of the twentieth century using the ECMWF forecasting system. Part II: Ensemble forecasts. Journal of Meteorological Applications12, 111–122.

Masselink, G., Pattiaratchi, C.B., 1998, The effect of sea breeze on beach morphology, surf zone hydrodynamics and sediment resuspension. Journal of Marine Geology 146, 115–135.

Papanastasiou, D.K., Melas, D., Lissaridis, I., 2010, Study of wind field under sea breeze conditions; an application of WRF model. Journal of Atmospheric Research 98, 102-117.

Pavía, E., Reyes, S., 1983, Variaciones espaciales y estacionales del viento superficial en la Bahía de Todos Santos, B.C., (In Spanish), Ciencias Marinas 9(1),151-167.

Ponce de León, S., Guedes Soares, C., 2010, The sheltering effect of the Balearic Islands in the hindcast wave field. Ocean Engineering 37, Issue 7, May 2010, 603-610. doi: 10.1016/j.oceaneng.2010.01.11.

Ponce de León S., Orfila A., Gómez-Pujol Ll., Renault L., Vizoso G., Tintoré J., 2011, Assessment of wind models around the Balearic Islands for operational wave forecast. Journal of Aplied Ocean Research (under review).

Ramis, C., Jansá, A., Alonso, S. 1990, Sea breeze in Mallorca. A numerical study. Journal of Meteorology and Atmospheric Physics 42, 249-258.

Ris, R.C., 1997, Spectral modelling of wind waves in coastal areas. Communications on Hydraulic and Geotechnical Engineering, Delft University of Technology PhD Thesis, 157 p.

Skamarock W.C., Klemp J.B., Dudhia J., Gill D.O., Barker D.M., Duda M.G., Huang X.Y., Wang W., Powers J.G., 2008, A Description of the Advanced Research WRF Version 3, NCAR Technical Note 475, 113 pp.

Skamarock W.C., Klemp J.B., Dudhia J., Gill D.O. , Barker D.M. , Wang W., Powers J.G., 2005, A description of the Advanced Research WRF version 2, NCAR Technical Note 468, 88 pp.

Simmons A., 2006. Observation, assimilation and the improvement of Global Weather Prediction-Some Results From Operational Forecasting and ERA-40, in

Predictability of Weather and Climate, Cambridge University Press, pp. 428-528.

Sonu, C.J., James, W.R., 1973, A Markov model for beach profile changes. Journal of Geophysical Research 78, 1462–1471.

Sotillo M.G. , Alvarez Fanjul E., Castanedo S., Abascal A.J., Menendez J., Emelianov M., Olivilla R., García-Ladona E., Ruiz-Villarreal M., Conde J., Gómez M., Conde P., Gutierrez A.D., Medina R., 2008, Towards an operational system for oil-spill forecast over Spanish waters: Initial developments and implementation test, Marine Pollution Bulletin 56, 686-703.

The WISE Group: Cavaleri L., Alves J.H.G.M. , Ardhuin F., Babanin A., Banner M., Belibassakis K., Benoit M., Donelan M., Groeneweg J., Herbers T.H.C., Hwang P., Janssen P.A.E.M., Lavreno I.V., Magne R., Monbaliu J., Onorato M., Polnikov V., Resio D., Rogers W.E., Sheremet A., McKee Smith J., Tolman H.L., Van Vledder G., Wolf J, Young I., 2007, Wave modelling. The state of the art, J. Prog. Oceanogr. 75, 603-674.

Yang X., Kmit M., Petersen C, Nielsen N.W., Sass B.H., Amstrup B., 2005. The DMI-HIRLAM upgrade in November 2005, DMI Technical Report, 05-15.

**Table 1 Geographical location of buoys and depths.**

| | Dragonera (B1) | Enderrocat (B2) |
|---|---|---|
| Latitude ($^o$N) | 39.55 | 39.49 |
| Longitude ($^o$E) | 2.10 | 2.703 |
| Depth (m) | 135 | 20 |

**Table 2 Numerical parameters of the performed simulations**.

| Parameters | Coarse gris | Nested grid |
|---|---|---|
| Third Generation wave model versions | WAM 4.52 | SWAN 4072 |
| Integration and source function time steps (seconds) | 120 seconds | 30 and 5 minutes |
| Spatial resolution ($^o$) (m) | 0.25$^o$ (25000 m) | 0.0125$^o$ (1500 m) |
| Number of points (NGXxNGY) | 11245(173x65) | 18281(181x101) |
| Lowest & Highest frequency (Hz) | 0.04177248 & 0.42 | 0.04177248 & 1 |
| Frequencies | 24 | 34 |
| Directions | 25 | 36 |
| Propagation | spherical | spherical |
| Type of model | deep water | shallow water |
| Latitudes, $^o$N | 30;46 | 39;40.25 |
| Longitudes, $^o$E | 37 | 1.75;4.0 |
| Longitudes, $^o$W | 6 | - |

**Table 3 Performed simulations with SWAN model.**

| Atmospheric model | dx=dy [º, km] | wind input time step | Wave output time step | Period of simulation |
|---|---|---|---|---|
| HIRLAM | 0.16º 16 km | 3 | 3 | August 2010 |
| WRF | 0.0173º 1.5 km | 1 | 1 | July and August 2009 |
| ECMWF | 0.125º 13 km | 6 | 6 | July 2009 |

**Table 4 Hourly description of the wind and sea state during 26$^{th}$ of July 2009 from 11 UTC up to 22 UTC for Alcudia and Palma Bays (U10-WRF wind speed above 10 m level of the sea; Hs-SWAN significant wave height [m]; φ and θ- wind and wave directions, respectively [degrees], nautical convention-the direction where the wave or wind come from, measured clockwise from the geographical North).**

| Location | Palma Bay | | Alcudia Bay | |
|---|---|---|---|---|
| Time(UTC) | Wind (U10;φ) | Waves (Hs;θ) | Wind (U10; φ) | Waves (Hs;θ) |
| 11 | 5 m/s ; S, SW | calm sea state | 7 m/s; NE | 0.65 m; NE |
| 12 | 6 m/s; S, SW | calm sea state | 9.2 m/s; NE | 0.65 m; NE |
| 13 | 6 m/s; S, SW | calm sea state | 9.2 m/s; NE | 0.65 m; NE |
| 14 | 6 m/s; S, SW | 0.3 m; SE; SW | 7.9 m/s; NE | 0.6 m; NE |
| 15 | 7 m/s; SE, S | 0.4 m; SE; S | 9 m/s; NE | 0.7 m; NE |
| 16 | 7 m/s; S, SW | 0.55 m; SE | 8.2 m/s; SE | 0.65 m; NE |
| 17 | 6.6 m/s; SE, SW | 0.5 m; SE | 7.7 m/s; SE | 0.6 m; NE |
| 18 | 6.6 m/s; SE, SW | 0.5 m; SE | 7.7 m/s; SE | 0.6 m; NE |
| 19 | 5.58 m/s; SE | 0.5 m; SE | 9.3 m/s; SE | 0.6 m; NE |
| 20 | 5 m/s; SE | 0.5 m; SE | 9 m/s; SE | 0.6 m; NE |

| | | | | |
|---|---|---|---|---|
| 21 | 4 m/s; SE | 0.4 m; SE | 9 m/s; SE | 0.5 m; NE |
| 22 | 2 m/s; E | 0.3 m; SE | 8.5 m/s; SE | 0.5 m; E |

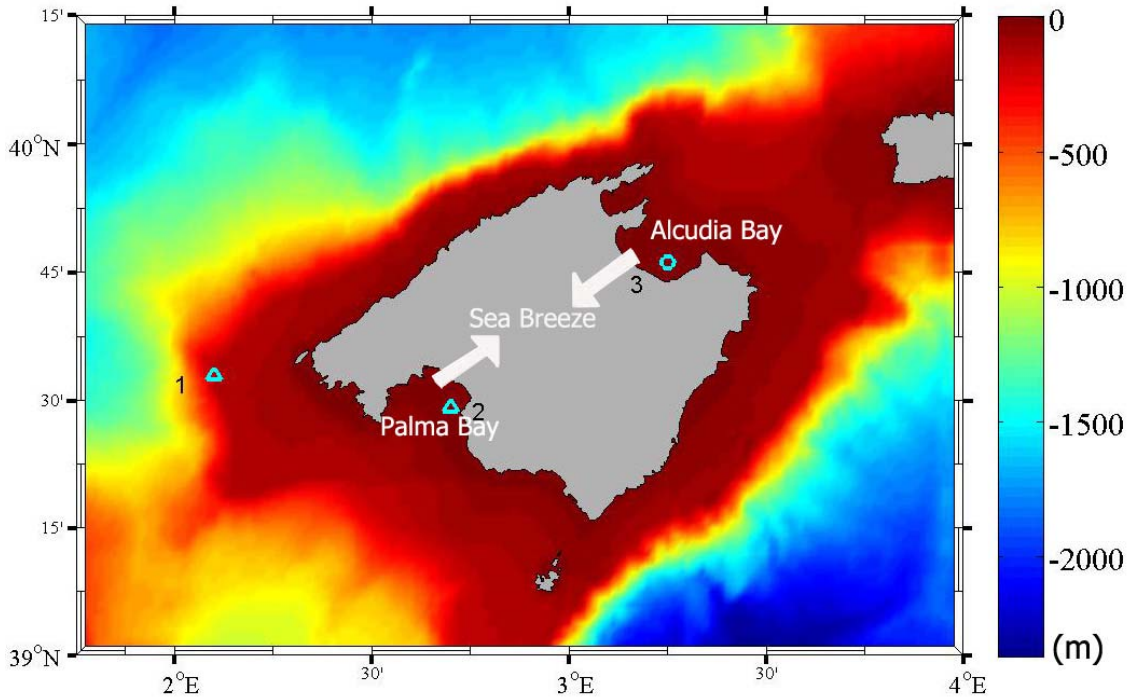


**Fig. 1 Bathymetry grid for the SWAN nested grid and the location of the buoys (triangles) and the output SWAN point (circle denoted with 3); 1-Dragonera (West); 2-Enderrrocat (Palma Bay); 3-Alcudia Bay.**

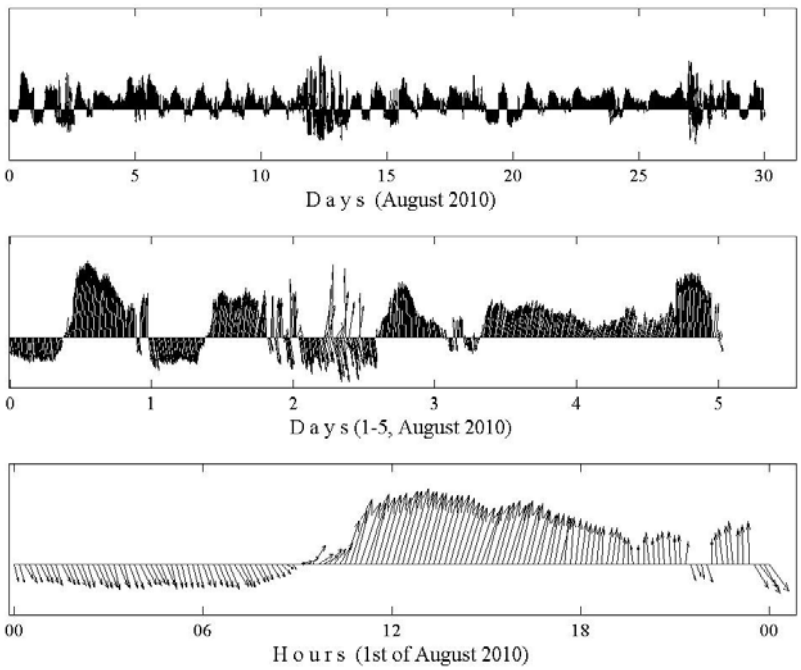


**Fig. 2 Measured (dt=10 minutes) breezes at Enderrocat. Top panel-30 days; middle panel-first five days of August; bottom panel-1st of August 2010.**

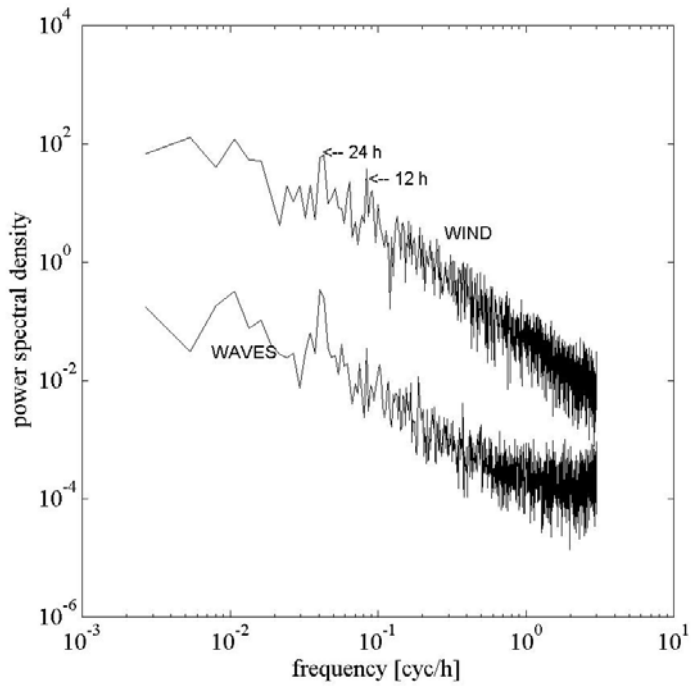


**Fig. 3 Power spectral density of wind speed and waves buoy measured signal for Enderrocat (August 2010). Arrows indicate spectral components of periods 24, 12, hours the low-frequency peaks are associated with diurnal and semidiurnal fluctuations.**

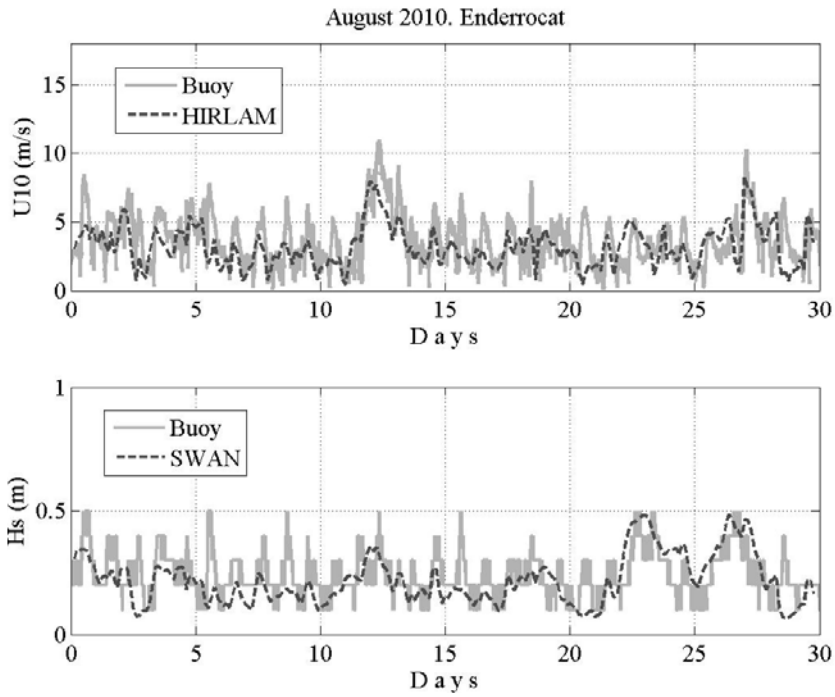


**Fig. 4 Time series comparison of the measured (buoy) and modelled (HIRLAM, dx=16 km) wind speed (top) and SWAN computed (bottom) Hs (m) at B2 at August 2010.**

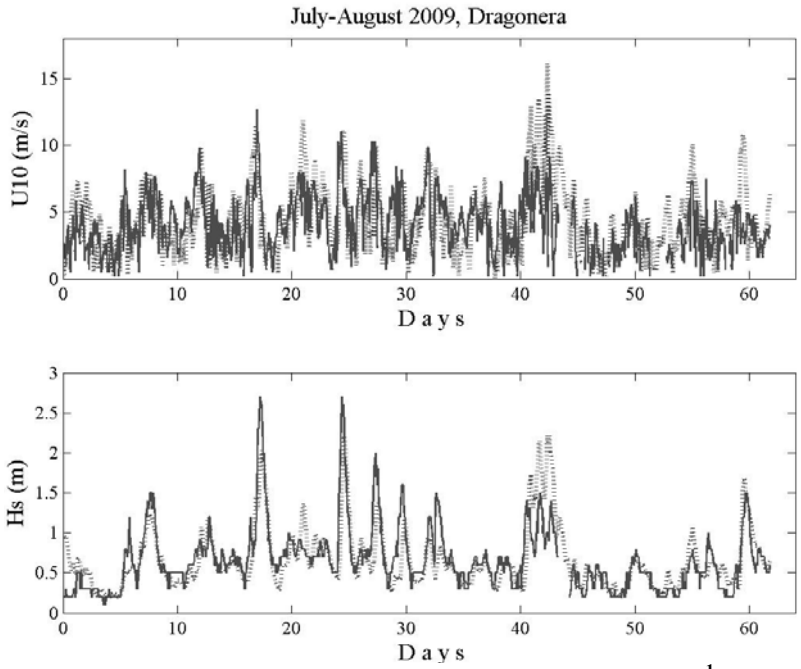


**Fig. 5 Time series (buoy- line) and WRF&SWAN (…) of the wind speed [ms$^{-1}$] at 10 m above the sea level (top) and the Hs [m] (bottom) at Dragonera during July and August 2009.**

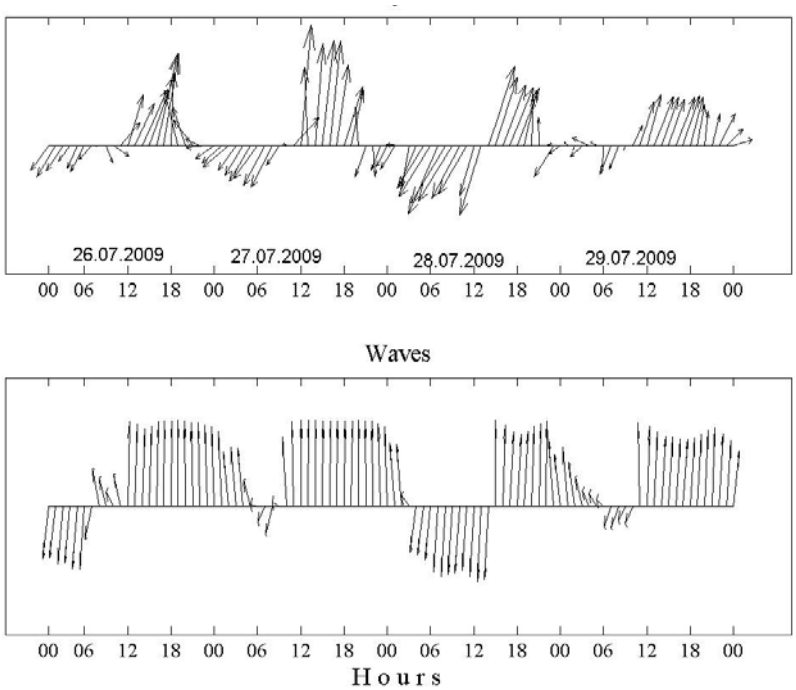


**Fig. 6 Hourly modelled WRF breezes wind directions (top) and the SWAN mean wave propagation (bottom) directions for 26$^{th}$-29$^{th}$ of July 2009 for B2.**

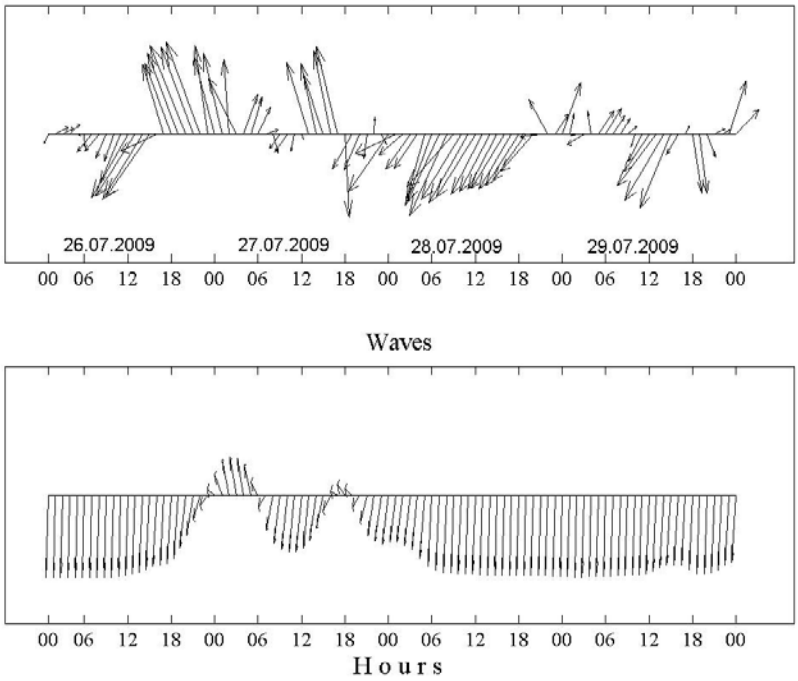


**Fig. 7 Hourly WRF breezes wind directions and the SWAN mean wave propagation directions for 26th of July 2009 at B3.**

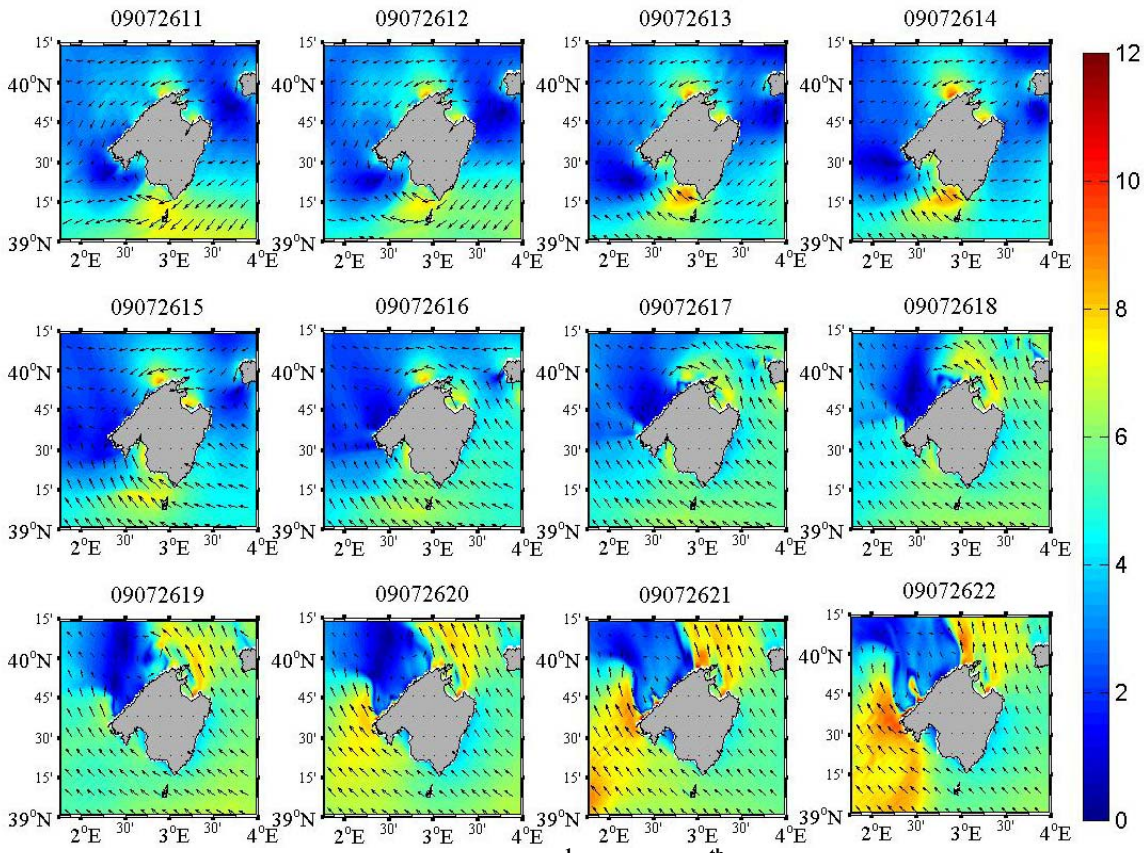


**Fig. 8 Hourly WRF wind fields (wind speed [$ms^{-1}$]) dated: 26th of July 2009 around the Mallorca Island.**

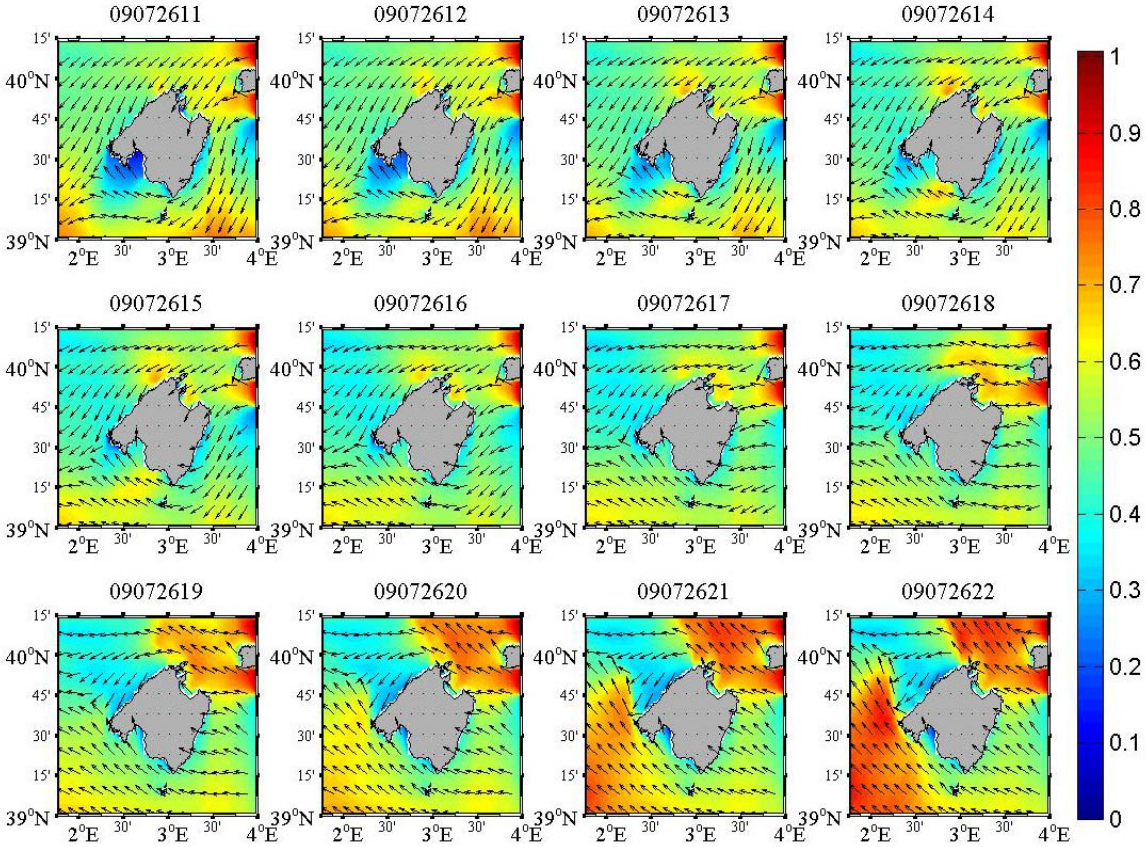


**Fig. 9 Hourly SWAN computed Hs [m] maps for the date: 26th of July, 2009.**

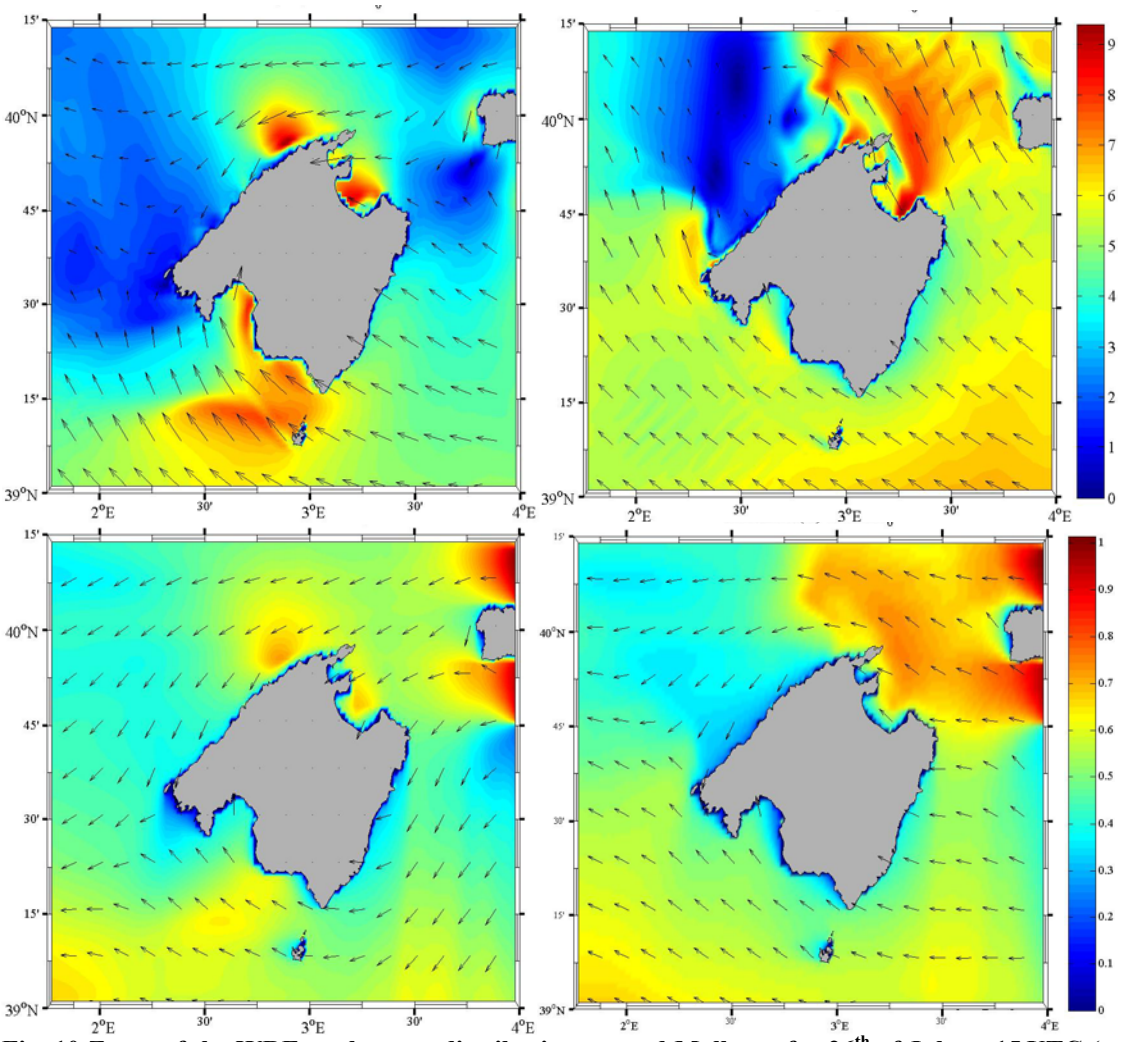


**Fig. 10 Zoom of the WRF sea breezes distribution around Mallorca for 26th of July at 15 UTC (top left) and 19 UTC (top right) UTC, respectively; bottom-SWAN computed Hs fields with 5 minutes time step (left-15 UTC; right-19 UTC).**

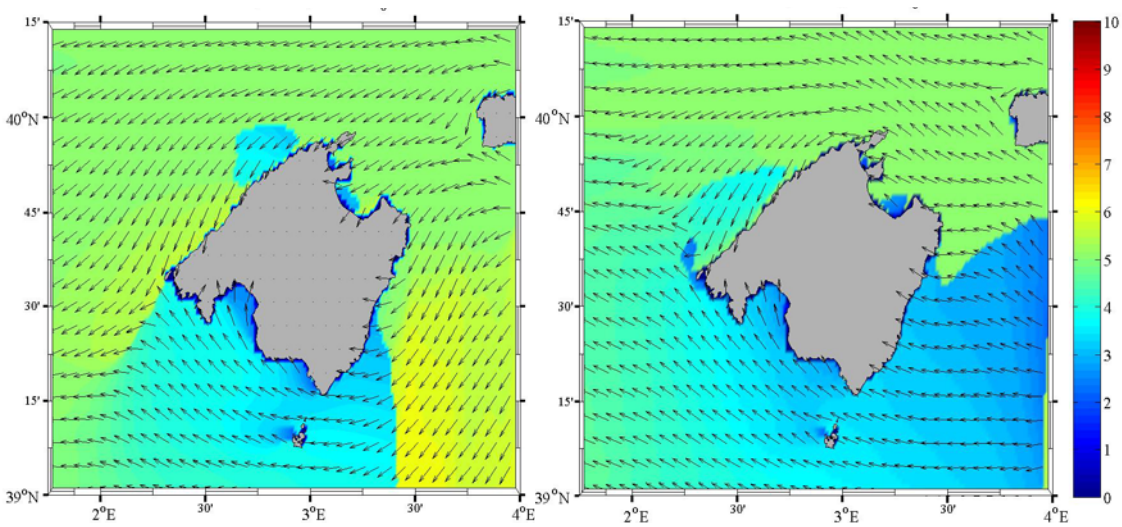


**Fig. 11 SWAN peak period (seconds) maps associated with the sea breezes. Dates: 26th of July of 2009 at 15 (left) and 19 UTC (right).**

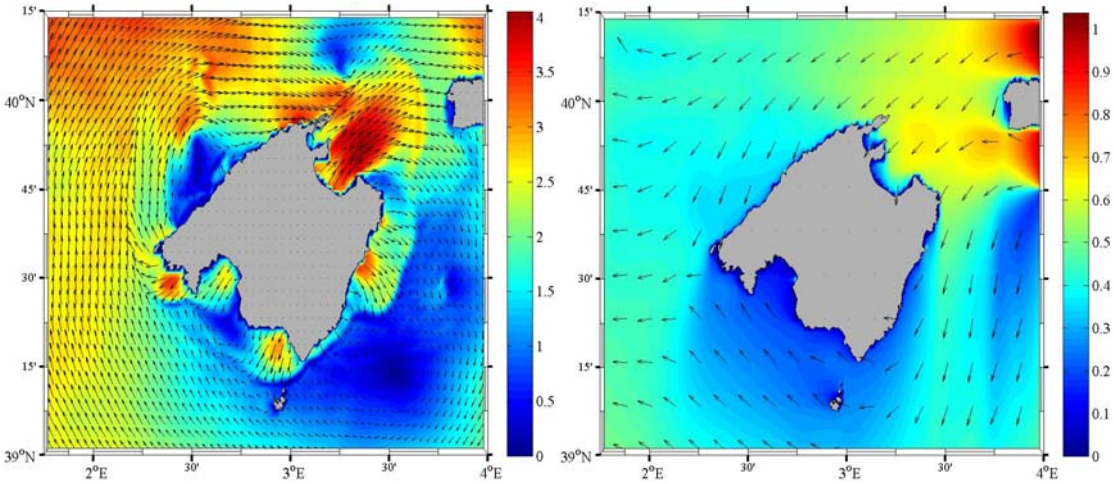


**Fig. 12 WRF wind field (wind speeds in m/s) representing the land breezes around the Mallorca Island for the date: 5th August, 2009 at 06 UTC (left panel), and the corresponding SWAN Hs (m) wave field (right panel).**

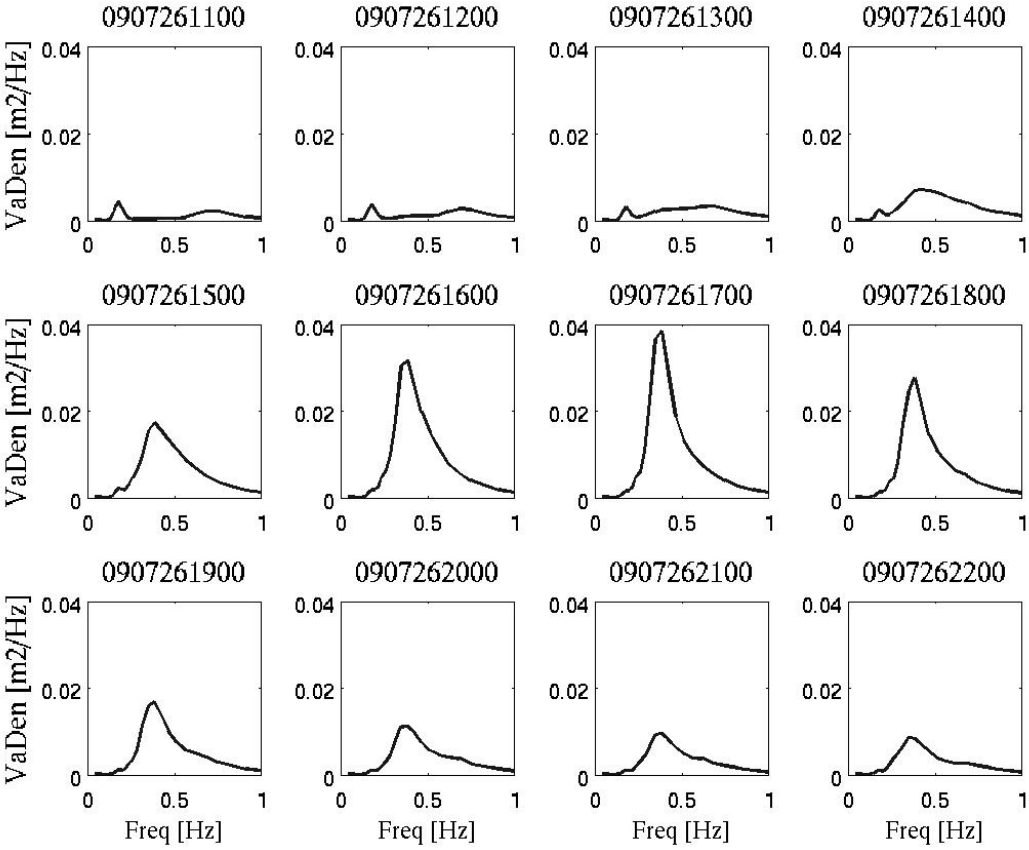


**Fig. 13 Hourly SWAN wave 1d variance densities (VaDen in [$m^2Hz^{-1}$]) spectra for 26th of July 2009 at B2 with WRF winds as a function of the frequencies (Freq [Hz]).**

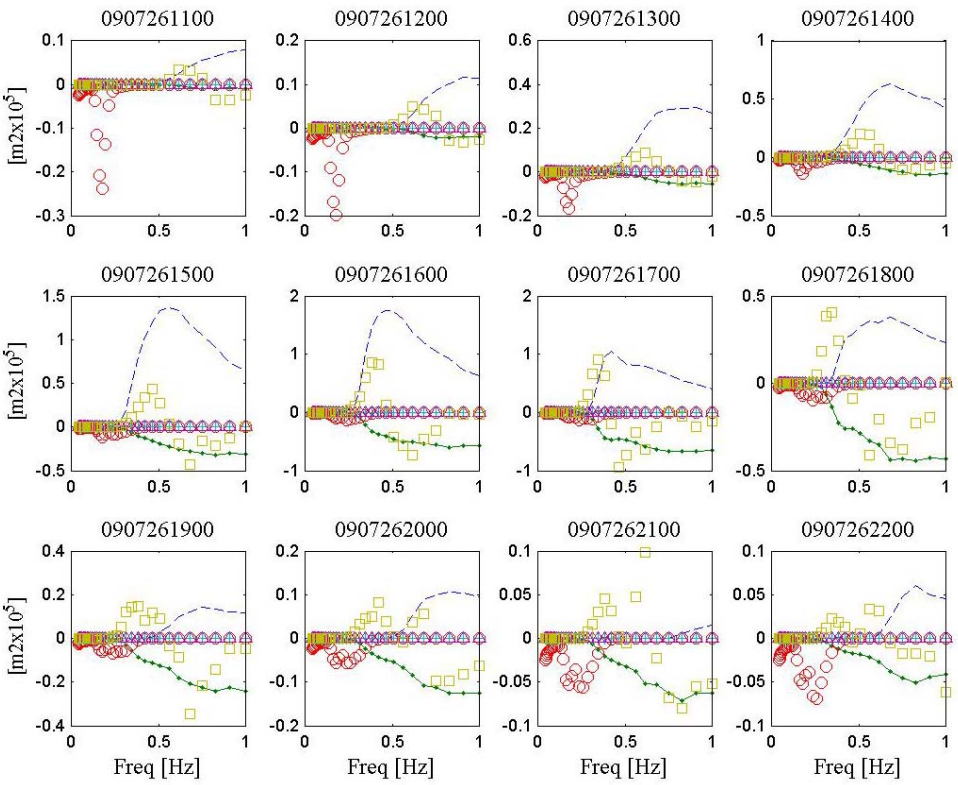


**Fig. 14 SWAN source functions [m$^2$] during the sea breezes of 26$^{th}$ of July 2009 at Enderrocat. (Swind-dashed line; Swcap-dashdot; Sfric-circle; Ssurf-plus; Snl3-triangle up; Snl4-squares; Freq=frequencies [Hz]).**

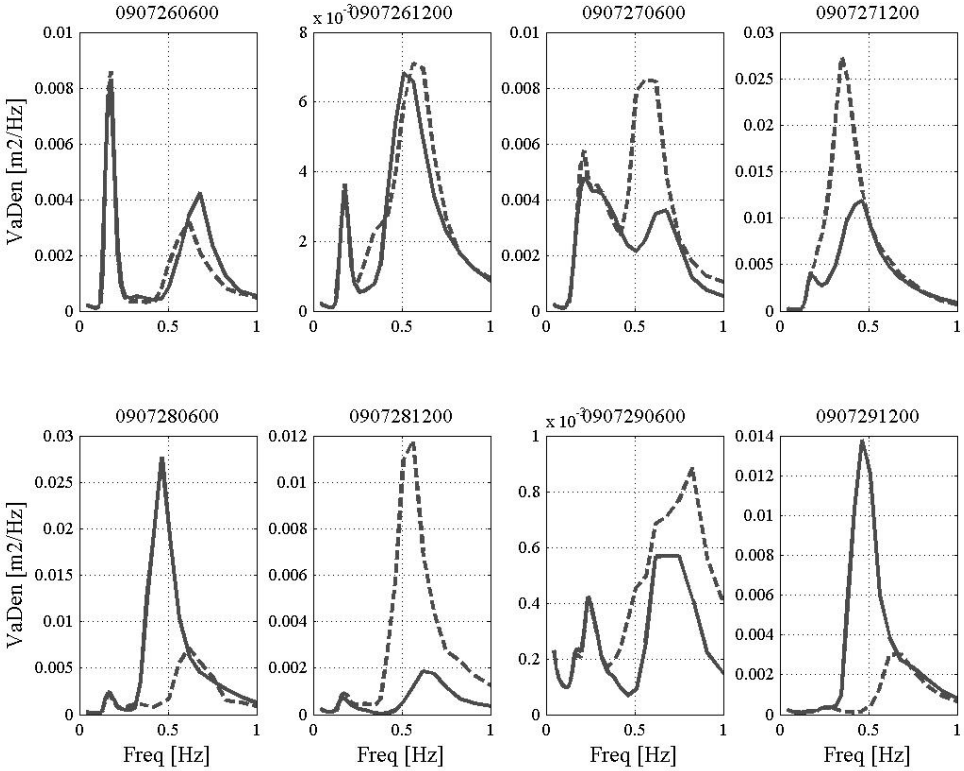


**Fig. 15 Computed SWAN one-dimensional wave spectra at B2 using the ECMWF(12.5)(solid line) and WRF(1.5)(dashed dot) during the breezes time of four days (26-29 of July 2009).**

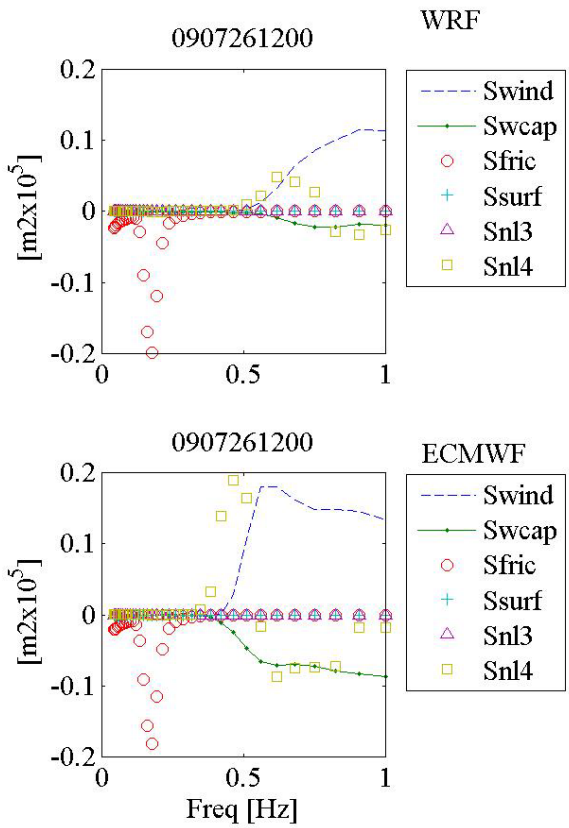


**Fig. 16 SWAN source functions [m$^2$] during the sea breezes of 26$^{th}$ of July 2009 at 12 UTC for Enderrocat. (Swind-dashed line; Swcap-dashdot; Sfric-circle; Ssurf-plus; Snl3-triangle up; Snl4-squares; Freq=frequencies [Hz]). Top- using the WRF winds; bottom-using the ECMWF winds.**

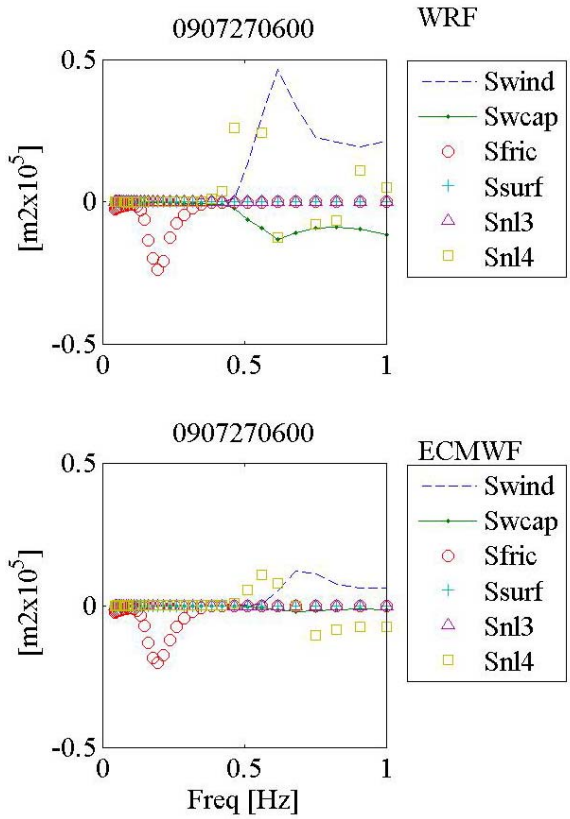


**Fig. 17 SWAN source functions [m$^2$] during the sea breezes of 27$^{th}$ of July 2009 at 06 UTC for Enderrocat. (Swind-dashed line; Swcap-dash dot; Sfric-circle; Ssurf-plus; Snl3-triangle up; Snl4-squares; Freq=frequencies [Hz]). Top- using the WRF winds; bottom-using the ECMWF winds.**